First-principles calculations of vacancy effects on structural and electronic properties of $TiC_x$ and $TiN_x$



2002 J. Phys.: Condens. Matter 14 10237

(http://iopscience.iop.org/0953-8984/14/43/320)

INSTITUTE OF PHYSICS PUBLISHING JOURNAL OF PHYSICS: CONDENSED MATTER

J. Phys.: Condens. Matter **14** (2002) 10237–10249 PII: S0953-8984(02)39531-6

# First-principles calculations of vacancy effects on structural and electronic properties of $TiC_x$ and $TiN_x$

**Z Dridi[1,2], B Bouhafs[1,2,3], P Ruterana[1] and H Aourag[2,4]**

[1] LERMAT, UMR6508-CNRS, ISMRA, 6, Bd du Maréchal Juin, F-14050 Caen Cedex, France
[2] LMSSM, Département de Physique, Faculté des Sciences, Université de Sidi-Bel-Abbès, 22000 Sidi-Bel-Abbès, Algeria

E-mail: bouhafs@ismra.fr

Received 16 July 2002
Published 18 October 2002
Online at stacks.iop.org/JPhysCM/14/10237

**Abstract**

First-principles calculations have been used to study the effect of vacancies on the structural and electronic properties in substoichiometric $TiC_x$ and $TiN_x$. The effect of vacancies on equilibrium volumes, bulk moduli, electronic band structures and density of states of the substoichiometric phases was studied using a full-potential linear augmented plane-wave method. A model structure of eight-atom supercells with ordered vacancies within the carbon and nitrogen sublattices is used.

We find that the lattice parameters of the studied stoichiometries in both $TiC_x$ and $TiN_x$ are smaller than that of ideal stoichiometric TiC and TiN. Our results for the variation of the lattice parameters and the bulk moduli for $TiC_x$ are found to be in good agreement with experiment. The variation of the energy gaps with the atomic concentration ratio shows that these compounds present the same trends. Results for $TiC_x$ are compared to a recent full-potential calculation with relaxed 16-atom supercells.

## 1. Introduction

Transition-metal (TM) carbides and nitrides have recently attracted much attention due to their interesting mechanical and physical properties. They are characterized by hardness, high melting point which classes them among the refractory compounds, excellent electrical and thermal conductivity, high chemical and thermal stability and good wear and corrosion resistance. All these properties make them suitable for many technological applications. Titanium carbide is used in cutting tools and in bulletproof vests, and is particularly attractive for aerospace applications. Titanium nitride is used as an electrically conducting barrier. This

[3] Author to whom any correspondence should be addressed.
[4] Permanent address: LERMPS, UTBM, Site de Sévenans, 90 010 Belfort Cedex, France.

  

combination of properties in TM carbides and nitrides has stimulated experimental [1–17] and theoretical studies [13, 15, 18–28] for the nature of bonding in these systems. This bonding has to be described as a mixture of three types of bonding, metallic, covalent and ionic [29], which simultaneously contribute to the cohesive energy.

Their technological importance has made them attractive for theoretical and experimental investigations. Titanium carbide is probably the most studied of the TM carbides, and often used as a prototype material for the studies of the other TM carbides [30–33]. However, both $TiC_x$ and $TiN_x$ compounds are nonstoichiometric and display deviations in stoichiometry over a wide range of composition. They are observed experimentally to crystallize in the cubic NaCl structure with carbon (nitrogen) atom vacancies (as many as 50%), which make the comparison between experiment and theory difficult.

Most of the works which study the effect of the vacancies on the properties have been carried out on $TiC_x$. From the experimental side, Chang and Graham [1] reported the elastic properties of $TiC_{0.91}$. Moisy-Maurice *et al* [2] presented an elastic diffuse neutron scattering study of the defect structure of $TiC_{0.76}$ and $NbC_{0.73}$. Guemmaz and his co-workers presented a series of studies on the nonstoichiometric $TiC_x$. Using ion beam synthesis, they studied the composition, nanoindentation [12] and electronic structure [13] of $TiC_x$. They also reported[15] a study of the elastic properties of the sub-stoichiometric $TiC_x$.

From the theoretical side, Redinger *et al* [20] using a self-consistent augmented plane wave (APW) method studied the substoichiometric $TiC_{0.75}$. Ivanovskii *et al* [21] using the LMTO–Green function method studied the metal and nonmetal substitutional impurities in TiC. Tan *et al* [34] using a tight-binding model studied structural relaxations in $TiC_x$, with carbon concentration $x = 0.5$–1. Guemmaz *et al* using the full-potential–linear muffin-tin orbital (FP–LMTO) investigated the elastic properties [15] and electronic structure [13] of $TiC_x$. Hugosson *et al* [18] using a combined approach of pseudopotential plane wave and FP–LMTO methods studied the phase stabilities and structural relaxations in $TiC_x$. The phase diagram for the vacancy-ordered structures in substoichiometric $TiC_x$ has been recently established from Monte Carlo simulations with long-range pair and multisite effective interactions, obtained from FP–LMTO calculations [28].

For substoichiometric TiN, only limited information has been published. From the experimental side, Höchst *et al* [3] presented a photoemission study of the electronic structure of $TiN_{0.99}$ and $TiN_{0.8}$. Jiang *et al* [5] reported the elastic constants and hardness of ion-beam sputtered $TiN_x$ films using Brillouin scattering and depth-sensing indentation. Kim *et al* [10] using line-focus acoustic microscopy measured the elastic constants of single-crystal titanium nitride films. Guemmaz *et al* [11] studied titanium nitrides synthesized by high-dose ion implementation. Theoretically, Capkova and Skala [22] studied the relaxations around vacancies and the chemical bonding of $TiC_x$ and $TiN_x$. Jhi and Ihm [23] studied the structural stabilities and the electronic structure of $TiC_xN_{1-x}$. Also, Jhi *et al* [24, 26] reported the effects of vacancies on mechanical properties of $TiC_x$ and $TiN_x$.

In this paper, we investigate the effect of vacancies on the structural and electronic structure, over a large range of stoichiometry in $TiC_x$ and $TiN_x$ compounds, using the full-potential linear augmented plane-wave (FP–LAPW) method. For each compound, we examine the equilibrium lattice constants, the bulk moduli, the electronic band structures and the density of states (DOS). We focus attention on two points: first, the variation of the bulk moduli of these solids with vacancy concentration, which may be correlated with hardness. The second goal of this study is to make a detailed analysis of the band structure and DOS in order to explain the effect of the vacancies. We take into account ordering of the vacancy sites. Such a detailed all-electron study on the effects of vacancies over a large range of stoichiometry has not, to our knowledge, been done for $TiN_x$ before.

## 2. Computational details

In the following calculation, we have distinguished the Ti($1s^2 2s^2 2p^6$) and C and N($1s^2$) inner-shell electrons from the valence band electrons of the Ti($3s^2 3p^6 3d^2 4s^2$), C($2s^2 2p^2$) and N($2s^2 2p^3$) shells. We calculate the electronic structure in the framework of the FLAPW method using the WIEN code [35]. The exchange–correlation energy of the electrons is described in the local-density approximation (LDA) using the Perdew–Wang functional [36]. Basis functions were expanded in combinations of spherical harmonic functions inside nonoverlapping spheres surrounding the atomic sites (muffin-tin (MT) spheres) and as Fourier series in the interstitial region. In the MT spheres, the $l$-expansion of the nonspherical potential and charge density was carried out up to $l_{max} = 10$. In order to achieve energy eigenvalue convergence, we have expanded the basis function up to $R_{\mathrm{MT}} K_{\mathrm{MAX}} = 8$ (where $K_{\mathrm{MAX}}$ is the maximum modulus for the reciprocal lattice vector, and $R_{\mathrm{MT}}$ is the average radius of the MT spheres). We have used separation radii between valence states and core states of 2.0, 1.9 and 1.7 au for the Ti, C and N atoms, respectively and 64 $k$ points in the Brillouin zone, generated according to the Monkhorst–Pack scheme [37]. The semicore states (Ti 3s,Ti 3p) are described as a combination of plane waves and local orbitals [38]. The total energy was converged to $10^{-4}$ Ryd.

The nonstoichiometric titanium carbide and titanium nitride were simulated by substituting the nonmetal C (or N) atoms in a unit cell with vacancies in a NaCl structure with an fcc Bravais lattice with four Ti sites and four C (or N) sites. We have considered the vacancy distribution as periodic, while this is not the case in the experimental samples. These vacancies are described by the plane waves in the FP–LAPW method. In order to study the cubic phase for several stoichiometries, from $x = 1.00$ to 0.25, we have used small eight-atom $Ti_4C_{4-n}$ and $Ti_4N_{4-n}$ supercells ($n = 0$, 1, 2 and 3), which correspond to a $1 \times 1 \times 1$ supercell which has the size of the primitive fcc unit cell. In stoichiometric TiC we thus have $Ti_4C_4$. In nonstoichiometric $TiC_x$, the carbon atoms were gradually removed. We thus have $Ti_4C_3$ for $TiC_{0.75}$, $Ti_4C_2$ for $TiC_{0.50}$ and finally $Ti_4C_1$ for $TiC_{0.25}$. The same system for several vacancy concentrations was used for TiN. For a given number $n = 0, \ldots, 3$ of vacancies, different atomic configurations have been optimized structurally. Therefore, for a given number $n$ we usually study only a small number of different configurations in which the vacancies are not really randomly distributed. For each configuration and each atomic number $n$, the fundamental physical properties are determined. For all crystals considered here, with a given vacancy concentration, we compute equilibrium lattice constants and bulk moduli by fitting the total energy versus volume curves to the Murnaghan equation of state [39].

## 3. Results and discussion

### *3.1. Structural properties*

For titanium carbide and nitride our calculated values 4.27 and 4.18 Å (table 1), respectively, are in good agreement with the LDA values (4.25 and 4.16 Å) of Ahuja *et al* [25] using the FP–LMTO approach, but in disagreement with the values found by Grossman *et al* [27] (4.38 and 4.32 Å), and Jhi *et al* [23] (4.332 and 4.261 Å) using the pseudopotential plane wave approach and LDA, which are overestimated relative to experiment (4.33 Å [6, 15] and 4.24 [6]). Using GGA in their calculations, Guemmaz *et al* [15] found a surprising underestimated value of 4.313 Å for TiC, since, in contrast to the LDA, GGA often overestimates the lattice constant and underestimates the bulk modulus.

In table 1, we show our equilibrium lattice constants for $TiC_x$ and $TiN_x$ calculated using LDA, along with other results obtained by LDA and GGA [15, 18], using the FP–LMTO method.

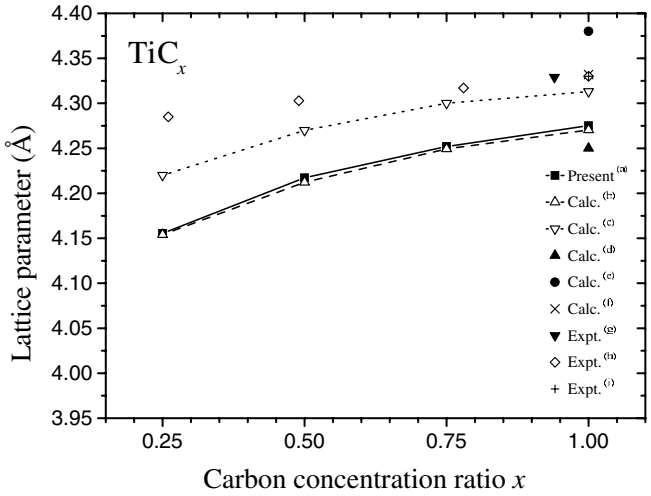


**Figure 1.** Variation of the lattice parameter as a function of the carbon concentration ratio $x$ for $TiC_x$. (a) Present calculations; (b) all-electron full-potential calculations of Hugosson *et al* [18]; (c) FP–LMTO calculations of Guemmaz *et al* [15]; (d) FP–LMTO calculations of Ahuja *et al* [25]; (e) pseudopotential plane-wave calculations of Grossman *et al* [27]; (f) pseudopotential plane-wave calculations of Jhi and Ihm [23]; (g) high-precision x-ray-diffraction measurements in $TiC_{0.94}$ [4]; (h) experimental values taken from [15]; (i) experimental values taken from [6].

**Table 1.** Calculated lattice constants (Å) for the substoichiometric $TiC_x$ and $TiN_x$ compounds compared to other theoretical results.

| | $TiC_x$ | | | $TiN_x$ |
|---|---|---|---|---|
| $x$ | Present | Reference [15] | Reference [18] | Present |
| 0.25 | 4.1554 | 4.22 | 4.1540 | 4.0904 |
| 0.5 | 4.2173 | 4.27 | 4.2122(4.2069) | 4.1330 |
| 0.75 | 4.2520 | 4.3 | 4.2493(4.2440) | 4.1625 |
| 1.0 | 4.2752 | 4.313 | 4.2704(4.2704) | 4.1813 |

Our results for the variation of the lattice constant as a function of the atomic concentration ratio $x$ of $TiC_x$ and $TiN_x$ are shown in figures 1 and 2, respectively, along with other theoretical and experimental results. From figures 1 and 2, one can note that the variation of the equilibrium lattice constant is not linear with vacancy concentration, which indicates that the Vegard rule is not valid for a compound with complex bonding properties. For $TiC_x$, we can make a comparison for the whole atomic concentration $0.25 \leqslant x \leqslant 1.0$ with the results of Guemmaz *et al* [15] using the FP–LMTO approach and Hugosson *et al* [18] using a combined approach of pseudopotential plane wave and FP–LMTO methods. Our calculated values for $TiC_x$ agree well with the values obtained for the eight-atom supercell by the recent all-electron full-potential calculations of Hugosson *et al* [18].

These compounds, in practice, are often not stoichiometric, but contain carbon or nitrogen vacancy defects. The comparison between theory and experiment for these classes of materials is often difficult because of the nonstoichiometry. The nonmetal vacancies cause displacements of the Ti atoms with respect to the rocksalt structure; this effect makes it difficult to directly compare the experimental data with theoretical results based on the ideal NaCl structure. High-precision x-ray-diffraction measurements [4] give a value of 4.329 Å for $TiC_{0.94}$.

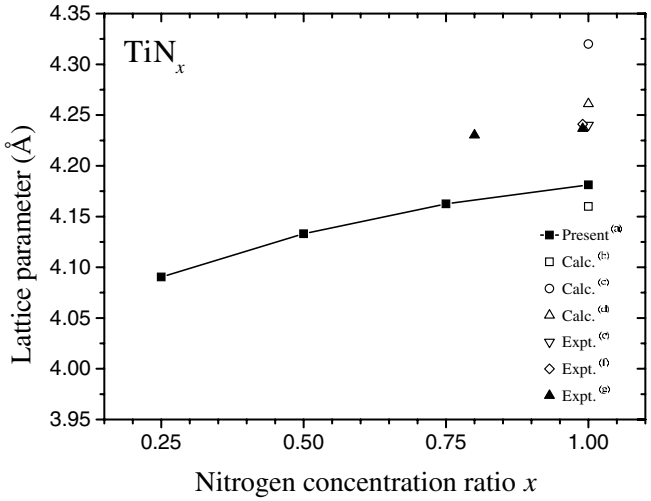


**Figure 2.** Variation of the lattice parameter as a function of the nitrogen concentration ratio $x$ for $TiN_x$. (a) Present calculations; (b) FP–LMTO calculations of Ahuja *et al* [25]; (c) pseudopotential plane-wave calculations of Grossman *et al* [27]; (d) pseudopotential plane-wave calculations of Jhi and Ihm [23]; (e) experimental values taken from [6]; (f) high-precision x-ray-diffraction measurements in $TiN_{0.99}$ [4]; (g) experimental values taken from [3].

Figure 1 indicates that our results are lower than the experimental data of Guemmaz *et al* [15] using x-ray diffraction for different stoichiometries, $TiC_{0.26}$, $TiC_{0.49}$, $TiC_{0.78}$ and TiC. We note that the lattice parameter increases with the carbon concentration from 4.15 Å for $TiC_{0.25}$ to 4.27 Å for TiC. The same trend is found in other experimental [15] and theoretical [15, 18] results. One can see from figures 1 and 2 that the introduction of vacancies in $TiC_x$ (or $TiN_x$) leads to a volume decrease. This is similar to what happens in pure TMs [40].

For $TiC_x$ the difference in theoretical and experimental volumes is of the order of 1% for TiC, 1.5% for $TiC_{0.75}$, 2% for $TiC_{0.50}$ and 3% for $TiC_{0.25}$. This is expected since the LDA is known to have this volume reducing effect, i.e., LDA overbinds. The relative volumes are changed very differently when introducing vacancies. The calculations also show good correspondence between theoretical and experimental equilibrium volumes.

For $TiN_x$ (see figure 2), the same behaviour is found as in the case of $TiC_x$. The lattice parameter increases with the nitrogen concentration ratio from 4.09 Å for $TiN_{0.25}$ to 4.18 Å for $TiN_{1.0}$. For comparison with experiment, we have reported in figure 2 the high-precision x-ray-diffraction measurements on $TiN_{0.99}$ of Dunand *et al* [4] which give a value of 4.241 Å. Other measurements [3] give nearly the same results for a small number of vacancies in $TiN_x$, 4.2301 Å for $TiN_{0.80}$ and 4.2366 Å for $TiN_{0.99}$.

Next, we report the bulk modulus evolution as a function of carbon and nitrogen concentration in $TiC_x$ and $TiN_x$, respectively. From our fitting of the total energies, we have also calculated the values of the bulk moduli and their pressure derivatives. The calculated bulk moduli of TiC and TiN are 277 and 317 GPa, respectively, which are overestimated relative to the experimental data, 233 GPa of [15] and 240 GPa from [1] for TiC and 318 from [10] for TiN. The pressure derivatives of the bulk moduli are found to be 4.11 and 4.59, for TiC and TiN, respectively. We can see from figure 3 and table 2 that our calculated bulk moduli for $TiC_x$ agree well with the LDA values of Hugosson *et al* [18] using both eight- and 16-atom supercells for all carbon concentrations $0.5 \leqslant x \leqslant 1.0$.

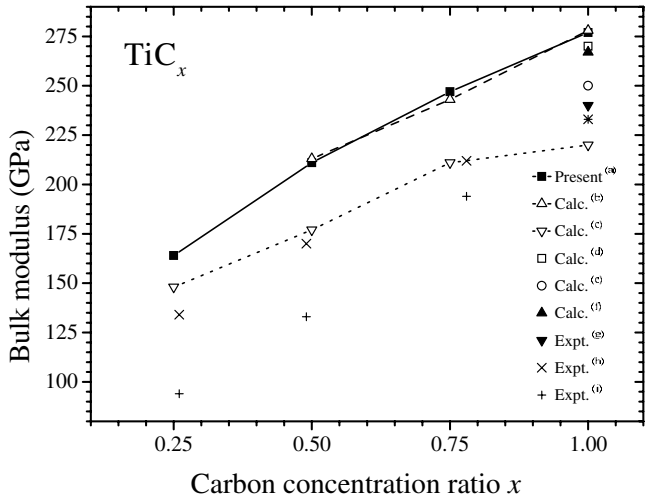


**Figure 3.** Variation of the bulk modulus as a function of the carbon concentration ratio $x$ for $TiC_x$. (a) Present calculations; (b) all-electron full-potential calculations of Hugosson *et al* [18]; (c) FP–LMTO calculations of Guemmaz *et al* [15]; (d) FP–LMTO calculations of Ahuja *et al* [25]; (e) pseudopotential plane-wave calculations of Jhi and Ihm [23]; (f) pseudopotential plane-wave calculations of Grossman *et al* [27]; (g) experimental values taken from reference [1]; (h) estimated by Guemmaz *et al* [15] from the measured Young moduli and $\nu$ taken as a linear interpolation between those of pure titanium ($\nu = 0.32$) and stoichiometric TiC ($\nu = 0.17$); (i) estimated by Guemmaz *et al* [15] from the measured Young moduli and $\nu$ taken as a constant equal to that of stoichiometric TiC ($\nu = 0.17$).

**Table 2.** Calculated bulk modulus $B_0$ (in GPa), and the derivative of the bulk modulus $B'$ for the substoichiometric $TiC_x$ and $TiN_x$ compounds compared to other theoretical results.

| | $TiC_x$ | | | | $TiN_x$ | |
|---|---|---|---|---|---|---|
| $x$ | $B_0$ | | | $B'$ | $B_0$ | $B'$ |
| 0.25 | 164[a] | 148[b] | | 3.92[a] | 183[a] | 3.00[a] |
| 0.50 | 211[a] | 177[b] | 213[c] | 4.07[a] | 233[a] | 3.02[a] |
| 0.75 | 247[a] | 211[b] | 243[c] | 3.49[a] | 274[a] | 4.97[a] |
| 1.0 | 277[a] | 220[b] | 278[c] | 4.11[a] | 317[a] | 4.59[a] |

[a] Using FP–LAPW method.
[b] FP–LMTO calculations of [15].
[c] Combined approach of pseudopotential plane wave and FP–LMTO calculations of [18]. The values are given for eight-atom supercells; those given in parenthesis are for 16-atom supercells.

The calculated bulk moduli of TiC and TiN are also in good agreement with the LDA values (270 and 310 GPa) of Ahuja *et al* [25], and a little bit higher than those of Grossman *et al* [27] (267 and 304 GPa) and Jhi and Ihm [23] (250 and 297 GPa). The value of 220 GPa of Guemmaz *et al* [15] for TiC is underestimated because of the use of GGA which underestimates the bulk modulus.

Our results show that increasing the carbon and the nitrogen concentration ratio in both $TiC_x$ and $TiN_x$, respectively, leads to larger $B_0$. $TiN_x$ has a larger bulk modulus than $TiC_x$ for all N or C concentration ratios.

Bulk moduli for $TiC_x$ have been estimated from the measured Young modulus $E$ by Guemmaz *et al* [15], and the Poisson coefficient $\nu$ through the relation [41] $B_0 = E/3(1-2\nu)$,

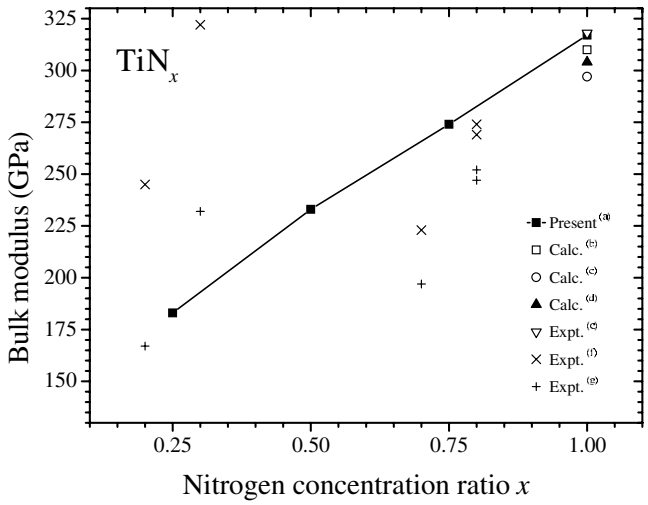


**Figure 4.** Variation of the bulk modulus as a function of the nitrogen concentration ratio $x$ for $TiN_x$. (a) Present calculations; (b) FP–LMTO calculations of Ahuja *et al* [25]; (c) pseudopotential plane-wave calculations of Jhi and Ihm [23]; (d) pseudopotential plane-wave calculations of Grossman *et al* [27]; (e) experimental values taken from [10]; (f) estimated from the measured Young moduli obtained by Jiang *et al* [5] with $\nu$ taken as a linear interpolation between those of pure titanium ($\nu = 0.32$) and stoichiometric TiN ($\nu = 0.20$); (g) estimated from the measured Young moduli obtained by Jiang *et al* [5] with $\nu$ taken as a constant equal to that of stoichiometric TiN ($\nu = 0.20$).

assuming these compounds are elastically isotropic. Unfortunately, no work concerning the variation of the Poisson coefficient with the carbon concentration is available. They have made two estimations: first using the Poisson coefficient as a constant equal to that of stoichiometric TiC ($\nu = 0.17$); second using a linear interpolation of the value of this coefficient between the pure titanium value ($\nu = 0.32$) and the stoichiometric TiC value ($\nu = 0.17$). They justified this linear interpolation by the fact that the Poisson coefficient is an elastic property of matter, as the Young modulus is.

Our calculation indicates that the bulk modulus increases with the carbon concentration from 164 GPa for $TiC_{0.25}$ to 277 GPa for $TiC_{1.0}$, values which are larger than those of Guemmaz *et al* [15] due to LDA. The linear fit of the variation of the bulk modulus versus nitrogen concentration gives the following equations:

$B(\text{GPa}) = 129 + 148x$ our calculations;

$B(\text{GPa}) = 43 + 191x$ from [15] with $\nu$ constant;

$B(\text{GPa}) = 102 + 135x$ from [15] with $\nu$ interpolated between Ti and stoichiometric TiC.

For $TiN_x$ the variation of the bulk modulus with the atomic concentration ratio is shown in figure 4. The behaviour is similar as in $TiC_x$; the bulk modulus increases with the nitrogen concentration from 183 GPa for $TiN_{0.25}$ to 317 GPa for TiN. The behaviour was found in the experimental values estimated from the measured Young moduli obtained by Jiang *et al* [5] from 172 GPa for $TiN_{0.25}$ to 282 GPa for TiN when $\nu$ was taken as constant and equal to that of stoichiometric TiN ($\nu = 0.20$), and from 242 GPa for $TiN_{0.25}$ to 286 GPa for $TiN_{1.0}$ when $\nu$ was taken as a linear interpolation between those of the pure titanium ($\nu = 0.32$) and the stoichiometric TiN ($\nu = 0.20$).

The linear fit of the variation of the bulk modulus versus nitrogen concentration leads to the following equations:

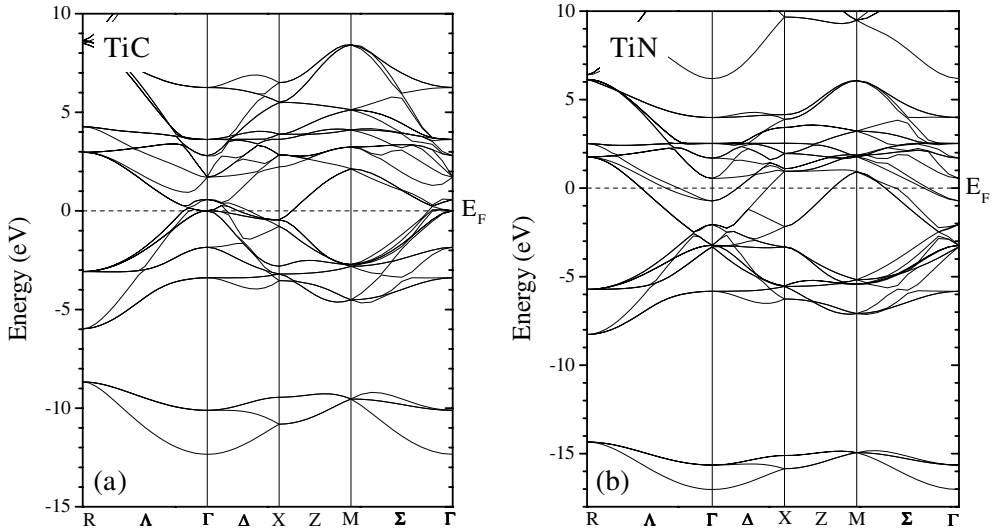


**Figure 5.** LDA band structures along the principal high-symmetry directions in the Brillouin zone calculated at the predicted equilibrium volumes for (a) $TiC_{1.0}$ and (b) $TiN_{1.0}$. The energy zero is taken at $E_F$.

$B(\text{GPa}) = 140 + 177x$ our calculations;

$B(\text{GPa}) = 135 + 147x$ from [5] with $\nu$ constant;

$B(\text{GPa}) = 228 + 58x$ from [5] with $\nu$ interpolated between Ti and stoichiometric TiN.

At high vacancy concentration, the electronic structure is deeply modified where new chemical bonds are then responsible for changes in the cohesion of the considered substoichiometric compounds. As a consequence of the formation of Ti-vacancy–Ti bonds, the bulk modulus decreases as a function of the vacancy concentration.

### *3.2. Electronic band structures*

Figure 5 shows the electronic band structures of stoichiometric TiC and TiN compounds, respectively. The electronic band structure is composed of several bands. At the bottom, far from the Fermi level, the band structure shows first deep narrow bands with low dispersion, which are mainly built of the nonmetal C 2s and N 2s states with a small contribution of the Ti 3d states for $TiC_{1.0}$ and $TiN_{1.0}$, respectively. An indirect energy gap of 2.69 eV for TiC and 6.07 eV for TiN separates these states from a series of bands containing C (N) 2p and Ti 3d states. However the main hybridization in this energy window concerns Ti 3d and C (N) 2p states. Just below the Fermi level, there are overlapping bands which originate from the nonmetal C 2p for TiC and N 2p states for TiN and contain also appreciable Ti 3d states. At higher energies, above the Fermi level, overlapping bands which are derived from the Ti 3d states appear which are mostly mixed with C 2p or N 2p states. The remainder of the valence states are separated by a wide gap from the occupied states, indicating strong covalent behaviour. These unoccupied states are largely of Ti d character and have been identified as either nonmetal C (N) 2p–Ti 3d antibonding states [29].

In the case of $TiN_x$, the main difference from TiC is that the electronegativity of nitrogen is higher than that of carbon. Thus the bands associated with nitrogen are lower in energy and narrower. The N 2s–Ti 3p band located below $-17$ eV is only 2.68 eV in width (figure 5(b)).

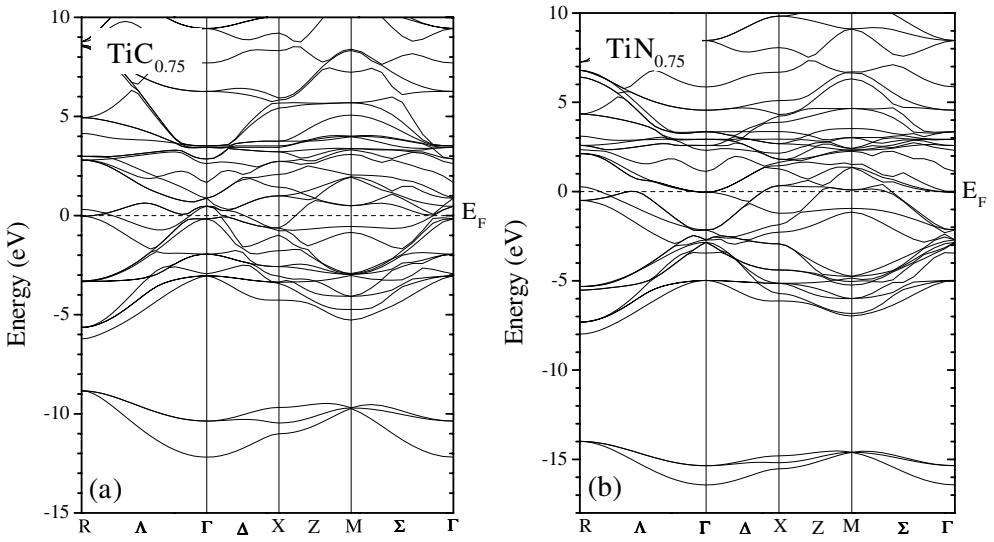


**Figure 6.** LDA band structures along the principal high-symmetry directions in the Brillouin zone calculated at the predicted equilibrium volumes for (a) $TiC_{0.75}$ and (b) $TiN_{0.75}$. The energy zero is taken at $E_F$.

The energy gap between N 2s–Ti 3p and N 2p–Ti 3d states is equal to 6.07 eV and much larger than in the C 2s–Ti 3p and C 2p–Ti 3d case. Thus the Ti 3d states are also globally shifted to lower energy. The C or N 2p bands overlap with the Ti 3d bands, and this overlap varies from TiC to TiN. It is stronger for TiC than for TiN. This suggests that the metal-to-metal bonding is similar in TiC and in TiN while the metal-to-nonmetal bonding is greater in TiC than in TiN, and it causes the top of the valence band to move up in energy.

The electronic band structure of $TiC_x$ and $TiN_x$ is shown for $x = 0.75$ in figure 6. From this figure we see that for TiC (TiN) the C (N) 2s bands remain narrow and inactive in the bonding of these materials, but the C (N) 2s–Ti 3p states are shifted to higher energies with increasing vacancy concentration ratio (see figures 7 and 8). Covalent C 2p–Ti 3d and N 2p–Ti 3d bonds were present in $TiC_x$ and $TiN_x$ and were found to be an important factor in determining equilibrium lattice constants and bulk moduli.

The band structures of $TiC_{1.0}$ and $TiC_{0.75}$ looked very much the same, with small shifts in band positions when we decrease the carbon concentration to $x = 0.75$. The C 2s band is seen to be still quite narrow, although there are now three carbon atoms per unit cell. However, the appearance of the vacancies leads to local perturbations of the electronic band structure, which result in the formation of vacancy states in the vicinity of $E_F$. These vacancy states increase with the decrease of the carbon concentration $x$, and are formed by the Ti 3d states from broken Ti–C bonds. The same situation is found in the calculated band structures of $TiN_{1.0}$ and $TiN_{0.75}$. We can see from figures 7 and 8 that the removal of some atoms (C or N) results in a usual decrease in the width of the C 2s and N 2s bands from 3.67 eV for $TiC_{1.0}$ to 2.69 eV for $TiC_{0.25}$, and from 2.68 eV for $TiN_{1.0}$ to 2.02 eV for $TiN_{0.25}$ as shown in figures 7 and 8. The energy gap between the C 2s and C 2p bands in TiC and the N 2s and N 2p bands in TiN decreases with the decrease of the vacancy concentration from 3.55 eV for $TiC_{0.25}$ to 2.62 eV for $TiC_{0.75}$ and from 7.18 eV for $TiN_{0.25}$ to 6.00 eV for $TiN_{0.75}$. Between 0.75 and 1 the energy gap becomes quite constant.

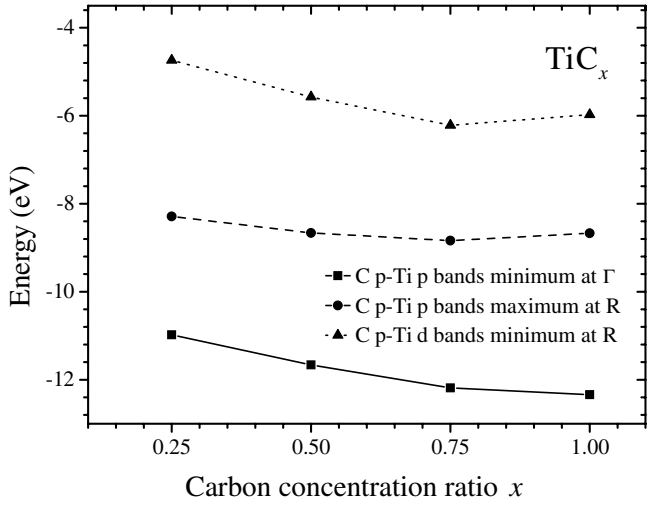


**Figure 7.** The variation of the C s–Ti p energy band minimum at Γ and the C s–Ti p energy band maximum and the C p–Ti d energy band minimum at R with the carbon concentration ratio $x$ in $TiC_x$.

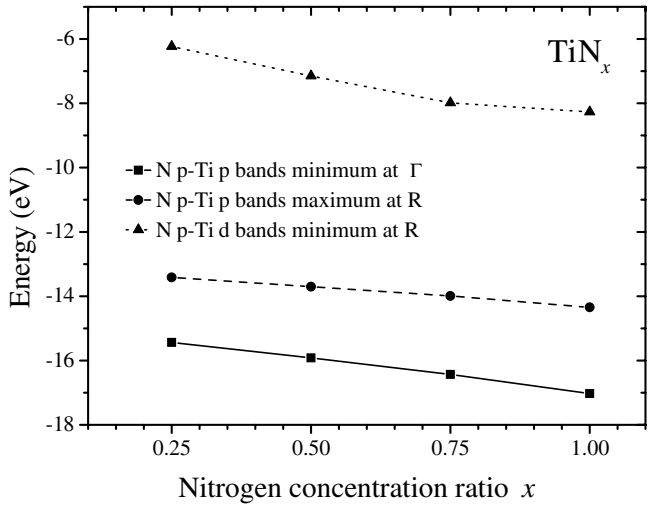


**Figure 8.** The variation of the N s–Ti p energy band minimum at Γ and the N s–Ti p energy band maximum and the N p–Ti d energy band minimum at R with the nitrogen concentration ratio $x$ in $TiN_x$.

### *3.3. Total and partial density of states*

We have also investigated the DOS of $TiC_x$ and $TiN_x$ to see whether they exhibit an increase in occupation of Ti d–Ti d states on creation of vacancies. In figure 9 we have displayed the calculated DOS for stoichiometric TiC and TiN. The TiC (TiN) DOS shows three main regions where the first region is predominantly C (N) s states with a small degree of hybridized Ti d states followed by a second region of strongly hybridized C (N) p and Ti d states representing the highly bonding part from −5.98 eV to the Fermi level for TiC and −8.26 to −2.66 eV for

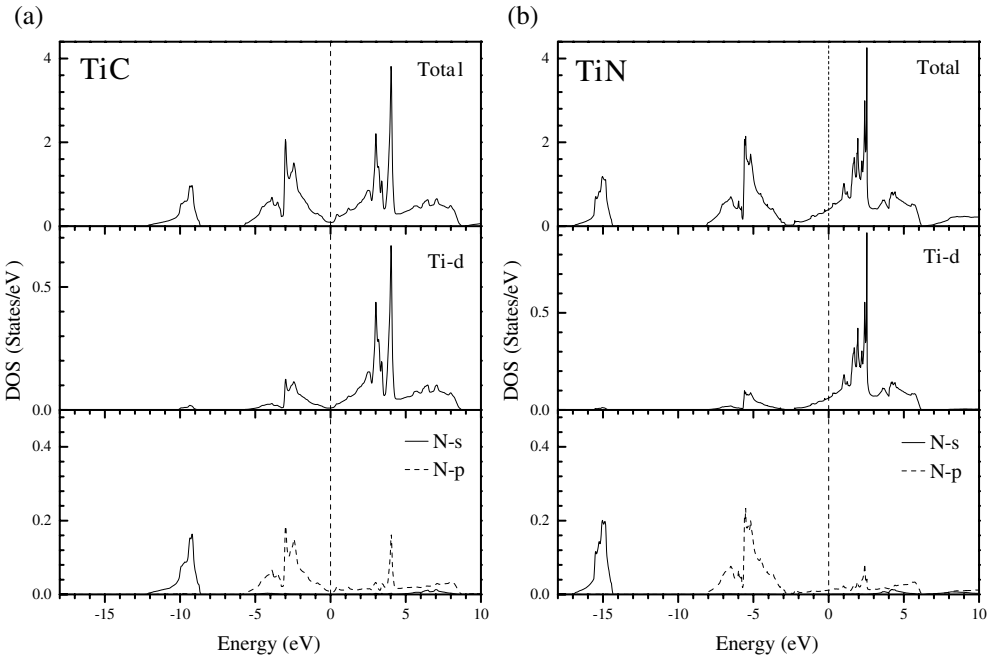


**Figure 9.** Total and partial DOS for (a) $TiC_{1.0}$ and (b) $TiN_{1.0}$. The Fermi level is indicated by a dashed line at zero energy.

TiN. Region III is predominantly Ti d states with a small degree of hybridized C (N) p states which correspond to the anti-bonding part. When vacancies are included, the changes in the DOS are clearly seen in figure 10 for $TiC_{0.75}$ and $TiN_{0.75}$. The first and second regions remain largely unchanged, with the peaks in region II becoming higher and more narrow. The large changes are found in region III where the entire character is changed. When the C (or N) atoms are removed, the electrons occupy Ti d states near the Fermi level. Some new pronounced peaks are seen to emerge below and around the Fermi level. In the second region, we found these peaks at $-1.86$ and $-0.64$ eV for TiC and $-0.93$ and 0 eV for TiN. These peaks are the so-called vacancy peaks which dominate at the Fermi level and are associated with Ti–Ti bonds through the vacancy site. These vacancy peaks are of mainly Ti d character and very localized. We note that $TiC_x$ and $TiN_x$ compounds exhibit similar features in the DOS. On the other hand, the larger difference of the electronegativity between C and N appears in the difference of the charge transfer, which is greater in $TiN_x$ than in $TiC_x$ and consequently a larger occupation of the Ti d–Ti d bonding states is found in $TiN_x$ than in $TiC_x$, when vacancies are included [24].

## 4. Discussion and conclusion

Using the FP–LAPW method, we have studied the behaviour of the lattice constants, bulk moduli and band structures with vacancy concentration in substoichiometric titanium carbides, and nitrides in the NaCl structure by using an eight-atom supercell. We see that the introduction of vacancies in $TiC_x$ and $TiN_x$ decreases the lattice constants and the bulk moduli; however, this variation is not linear. The observed variation of the lattice constants and bulk modulus as a function of vacancy concentration is found to be related to the evolution of chemical bonds.

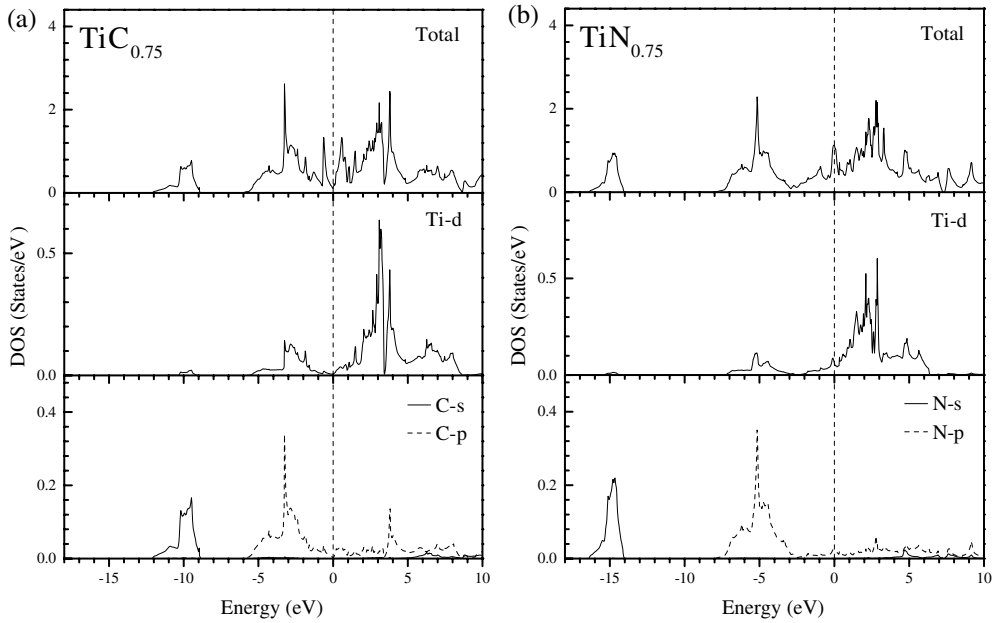


**Figure 10.** Total and partial DOS for (a) $TiC_{0.75}$ and (b) $TiN_{0.75}$. The Fermi level is indicated by a dashed line at zero energy.

We can deduce that these compounds become less rigid with the increase of the vacancy concentration.

We report also the variation of the band structure and DOS with vacancy concentration. There were similarities in the electronic band structure and DOS of these two compounds. The increase of the vacancy concentration is seen by the appearance of vacancy states in the band structure and vacancy peaks in the DOS below and around the Fermi level which are due to the d states from broken Ti–C (N) bonds and lead to less hard materials. We have found that $TiC_x$ and $TiN_x$ with different stoichiometries present similar trends.

Our calculations illustrate that a systematic consideration of the treatment of vacancies may help to identify patterns of their effects on the structural and electronic properties of TM carbides and nitrides. Finally, the behaviour obtained for both the lattice constant and bulk modulus indicates that the substoichiometric titanium carbides and nitrides, although completely ordered, are sufficiently realistic to provide agreement with experiment.

## Acknowledgments

This work is carried out with the support of the Algerian–French Ministries of Foreign Affairs under project CMEP 01 MDU 516. One of us (BB) would like to acknowledge the Islamic Development Bank (IDB) of the Kingdom of Saudi Arabia for financial support and the Abdus Salam ICTP (Trieste, Italy) for technical support.

## References

[1] Chang R and Graham L J 1966 *J. Appl. Phys.* **37** 3778
[2] Moisy-Maurice V, de Novion C H, Christensen A N and Just W 1981 *Solid State Commun.* **39** 661

[3] Höchst H, Bringans R D, Steiner P and Wolf Th 1982 *Phys. Rev.* B **25** 7183
[4] Dunand A, Flack H D and Yvon K 1985 *Phys. Rev.* B **31** 2299
[5] Jiang X, Wang M, Schmidt K, Dunlop E, Haupt J and Gissler W 1991 *J. Appl. Phys.* **69** 3053
[6] Zhukov V P, Gubanov V A, Jepsen O, Christensen N E and Andersen O K 1988 *J. Phys. Chem. Solids.* **49** 841 and references therein
[7] Hara T, Tani K, Inoue K, Nakamura S and Murai T 1990 *Appl. Phys. Lett.* **57** 1660
[8] D'Anna E, Leggieri G, Luches A, Martino M, Drigo A V, Mihailescu I N and Ganatsios S 1991 *J. Appl. Phys.* **69** 1687
[9] Katz A, Feingold A, Pearton S J, Nakahara S, Ellington M, Chakrabarti U K, Geva M and Lane E 1991 *J. Appl. Phys.* **70** 3666
[10] Kim J O, Achenbach J D, Mirkarimi P B, Shinn M and Barnett S A 1992 *J. Appl. Phys.* **72** 1805
[11] Guemmaz M, Mosser A, Raiser D, Grob J J, Cornet A and Paletto S 1995 *Mater. Res. Soc. Symp. Proc.* **354** 243
[12] Guemmaz M, Mosser A, Boudoukha L, Grob J J, Raiser D and Sens J C 1996 *Nucl. Instrum. Methods* B **111** 263
[13] Guemmaz M, Moraitis G, Mosser A, Khan M A and Parlebas J C 1997 *J. Electron Spectrosc. Relat. Phenom.* **83** 173
Guemmaz M, Mosser A and Grob J J 1997 *Appl. Phys.* A **64** 407
[14] Schmid P E, Sunaga M S and Lévy F 1998 *J. Vac. Sci. Technol.* A **16** 2870
[15] Guemmaz M, Mosser A, Ahujab R and Johansson B 1999 *Solid State Commun.* **110** 299
[16] Mah G, Nordin C W and Fuller J F 2000 *J. Vac. Sci. Technol.* **11** 371
[17] Juppo M, Alén P, Ritala M, Sajavaara T, Keinonen J and Leskelä M 2002 *Electrochem. Solid State Lett.* **5** C4
[18] Hugosson H W, Korzhavyi P, Jansson U, Johansson B and Eriksson O 2001 *Phys. Rev.* B **63** 165116
[19] Gelatt C D Jr, Williams A R and Moruzzi V L 1983 *Phys. Rev.* B **27** 2005
[20] Redinger J, Eibler R, Herzig P, Neckel A, Podloucky R and Wimmer E 1985 *J. Phys. Chem. Solids* **46** 383
[21] Ivanovskii A L, Novikov D L, Anisimov V I and Gubanov V A 1988 *J. Phys. Chem. Solids* **49** 5487
[22] Capkova P and Skala L 1992 *Phys. Status Solidi* b **71** 85
[23] Jhi S and Ihm J 1997 *Phys. Rev.* B **56** 13826
[24] Jhi S-H, Louie S G, Cohen M L and Ihm J 2001 *Phys. Rev. Lett.* **86** 3348
[25] Ahuja R, Eriksson O, Wills J M and Johansson B 1996 *Phys. Rev.* B **53** 3072
[26] Jhi S H, Ihm J, Louie S G and Cohen M L 1999 *Nature* **399** 132
[27] Grossman J C, Mizel A, Côté M, Cohen M L and Louie S G 1999 *Phys. Rev.* B **60** 6343
[28] Korzhavyi P A, Pourovskii L V, Hugosson H W, Ruban A V and Johansson B 2002 *Phys. Rev. Lett.* **88** 015505
[29] Blaha P and Schwarz K 1983 *Int. J. Quantum Chem.* **23** 1535
[30] Sorenson O T 1981 *Nonstoichiometric Oxides* (New York: Academic)
[31] Mandelcorn L 1981 *Non-Stoichiometric Compounds* (New York: Academic)
[32] Freer R (ed) 1990 *The Physics and Chemistry of Carbides, Nitrides, and Borides* (Dordrecht: Kluwer)
[33] Kosuge K 1994 *Chemistry of Nonstoichiometric Compounds* (Oxford: Oxford University Press)
[34] Tan K E, Bratkovsky A M, Harris R M, Horsfield A P, Nguyen-Mahn D, Pettifor D G and Sutton A P 1997 *Modell. Simul. Mater. Sci. Eng.* **5** 187
[35] Blaha P, Schwarz K and Luitz J 1997 *WIEN97, a Full Potential Linearized Augmented Plane Wave Package for Calculating Crystal Properties* Technical University of Vienna (ISBN 3-9501031-0-4)
This is an improved and updated Unix version of the original copyrighted WIEN code, which was published by Blaha P, Schwarz K, Sorantin P I and Trickey S B 1990 *Comput. Phys. Commun.* **59** 399
[36] Perdew J P and Wang Y 1992 *Phys. Rev.* B **45** 13244
[37] Monkhorst H J and Pack J D 1976 *Phys. Rev.* B **13** 5188
[38] Singh D 1991 *Phys. Rev.* B **43** 6388
[39] Murnaghan F D 1944 *Proc. Natl Acad. Sci. USA* **30** 5390
[40] Meyer B and Fahnle M 1997 *Phys. Rev.* B **56** 13595
[41] Noyan I C and Cohen J B 1987 *Residual Stress Measurement by Diffraction and Interpretation* (Berlin: Springer)
[42] Schwarz K and Blaha P 1983 *Local Density Approximations in Quantum Chemistry and Solid State Physics* ed J P Dahl and J Avery (New York: Plenum)